02

Cherenkov radiation and cathodoluminescence in diamond under the action of electrons with an energy of 5.7 MeV

© A.G. Burachenko[1,2], K.P. Artyomov[1,3], A.V. Vukolov[3], A.A. Krylov[1,2], E.I. Lipatov[1,2], V.S. Ripenko[1,2], A.S. Gogolev[3]

[1] Institute of High Current Electronics, Siberian Branch, Russian Academy of Sciences,
634055 Tomsk, Russia
[2] Tomsk State University,
634050 Tomsk, Russia
[3] Tomsk Polytechnic University,
634050 Tomsk, Russia

e-mail: bag@loi.hcei.tsc.ru

Received October 31, 2023
Revised December 4, 2023
Accepted December 8, 2023

The spectral and kinetic characteristics of the radiation of diamond samples with different impurity-defect compositions under the action of electrons with an energy of 5.7 MeV have been studied. Cherenkov radiation was obtained in all studied samples. A difference has been established in the radiation spectra of nominally pure samples obtained by different synthesis methods. A diamond sample has been determined that is suitable for registration of Cherenkov radiation in a wide spectral range (UV and visible) under conditions of low beam current density (tens of nA/cm^2).

Keywords: Cherenkov radiation, cathodoluminescence, diamond, electron beam, spectral and kinetic characteristics of the radiation.

DOI: 10.61011/EOS.2023.12.58176.5713-23

Introduction

Diamond is a promising material for detectors of ionizing radiation and high-energy particles that are sensitive in the UV region of the spectrum and capable of operating in conditions of high radiation background and high temperature [1,2]. In particular, diamond is a promising material for use as a radiator for Cherenkov detectors [3] in tokamaks [2] for detection of electrons with energies of tens to hundreds of keV and several MeV. In addition, the use of diamond in a Cherenkov detector for charged particles of the solar wind in near-Earth space is promising. The energy of solar-wind electrons also ranges from tens or hundreds of keV to several MeV [4]. It is known that, in addition to Cherenkov radiation (CR), luminescence can be produced in the radiator material of a Cherenkov detector at such energies of electrons [3]. This luminescence distorts the detector signal. In addition, various impurities present in diamond samples will contribute to emission. Therefore, studies of spectral and kinetic characteristics of emission of diamond samples with different impurity-defect compositions are relevant. The emission of diamond samples with different impurity-defect compositions was studied at electron energies of tens to hundreds of keV [5,6]. It was shown in these studies that the main contribution to emission of diamond samples was made by cathodoluminescence, and CR was not detected at the sensitivity level of the recording equipment.

The aim of the present work is to investigate the spectral and kinetic characteristics of emission of diamond samples with different impurity-defect compositions exposed to a beam of electrons with an energy of several MeV (5.7 MeV).

Experimental setup and methods

The emission study was carried out for four diamond samples. Their characteristics are presented in the table. Samples Nos. 1 and 2 were prepared by chemical vapor deposition, and samples Nos. 3 and 4 were fabricated using method of temperature gradient in high-pressure and high-temperature conditions (HPHT) [7].

The emission of diamond samples with different impurity-defect compositions was studied at the MI-6 microtron of Tomsk Polytechnic University [8–11]. The microtron generated an electron beam with an energy of 5.7 MeV, a macropulse duration of 0.5 μs, and a macropulse repetition rate of 25 Hz. The electron beam current was no more than 1 mA per pulse. The electron beam was focused on the target (diamond samples). The focal diameter of the electron beam was ~ 3 mm. The current density of the beam was ~ 20 A/cm^2.

The block diagram of the experimental setup is shown in Fig. 1. The samples were mounted on a metal holder with the plane pointing toward the electron beam. The holder could rotate around its axis with the help of a rotating platform with an electromechanical drive (produced by Standa), thus changing the angle of incidence of the electron beam onto the plane of the studied sample. Angle

Characteristics of the studied samples

Sample number	Synthesis method	Presence of impurities	Size, mm
№ 1	Chemical vapor deposition	Nominally pure	$5 \times 5 \times 0.25$
№ 2	Chemical vapor deposition	Nitrogen	$5.5 \times 3.2 \times 0.5$
№ 3	Temperature gradient	Nominally pure	$5 \times 5 \times 0.25$
№ 4	Temperature gradient	Nitrogen, NV centers, interstitials	$3.42 \times 6.44 \times 0.61$

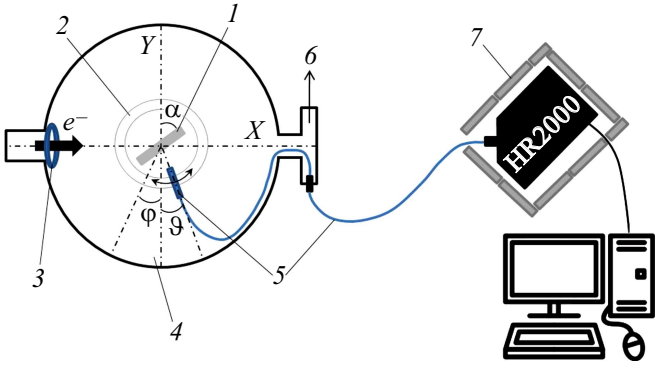

Figure 1. Block diagram of the experimental setup for recording the emission spectra of diamond samples: *1* — sample, *2* — rotating platform, *3* — induction current sensor, *4* — chamber, *5* — fiber, *6* — to turbomolecular pump, *7* — lead.

α between axis Y, which is perpendicular to the electron beam axis, and the sample plane was equal to 54° (Fig. 1) and remained unchanged in all experiments. The fiber was also mounted on a rotating platform that moved the fiber only in the azimuthal direction around the sample (Fig. 1). The distance from the center of the sample to the plane of the fiber was ~ 2 cm.

Since CR propagates at a certain angle to the direction of motion of charged particles and depends on their energy, the values of angles α and ϑ at which CR will hit the receiving part of the fiber were calculated for an electron beam with an energy of 5.7 MeV. The calculation was performed using the GEANT4 numerical code [12]. The values of angles α and ϑ were 54 and 5°, respectively. In contrast to CR, luminescence is emitted into a full solid angle (4π); therefore, in order to ensure that the emission spectrum has no or minimal CR contribution, the fiber was positioned at angle φ or at an even greater angle to axis Y. In most cases, it was sufficient to rotate the fiber by angle $\varphi = 15°$ to suppress completely or reduce significantly the CR contribution to the emission spectrum of the sample under investigation.

The spectral characteristics of emission were recorded using an HR2000+ES spectrometer (OceanOptics Inc.) with known spectral sensitivity in the wavelength range of 190–1100 nm (resolution, ~ 0.9 nm). Radiation from the sample was transmitted to the spectrometer via a quartz fiber, which was also transparent at 190–1100 nm. The kinetic characteristics of emission were studied with a MicroFJ-SMA-30035 silicon PMT sensitive in the wavelength range of 200–900 nm. The rise time of the transient response of the PMT was ~ 0.1 ns, and the microcell recharge time constant was 45 ns [13]. The distance from the sample plane to the fiber was the same as in the spectral studies. The design of the experiment on PMT measurements of the kinetic characteristics of emission was similar to that of measurements of the spectral characteristics (Fig. 1); the sole difference was that the PMT was installed instead of the spectrometer. The PMT signal was output to a Hantek DSO-6074BC (70 MHz, 1 GSa/s) oscilloscope. The kinetic characteristics of emission were investigated in different spectral ranges through the use of different optical filters: UFS-2 (260–380 nm), SS-8 (360–540 nm), ZhS-17 (480–3000 nm), and OS-12 (540–3000 nm). The beam current was recorded using an induction current sensor mounted at the output of the accelerator section (Fig. 1). However, due to the low temporal resolution of this sensor, it was only possible to monitor correctly the number of beam electrons. The beam current waveform corresponded to the oscillogram of current given in [11]. To reduce the influence of interference from bremsstrahlung radiation of the electron beam during operation, the spectrometer and the PMT were shielded with lead. The chamber was continuously evacuated by a turbomolecular pump, which provided a vacuum no worse than 10^{-6} Torr. The studies of emission of diamond samples were carried out at room temperature.

Experimental results and discussion

Spectral characteristics of emission of diamond samples

The emission and transmission spectra of all four studied samples are shown in Figs. 2–4. Cherenkov radiation is observed in the emission spectrum of low-impurity diamond sample No. 1 when the fiber is rotated by angle θ. No cathodoluminescence was observed in the emission spectra for this sample when the fiber was rotated by different angles, including ϑ and φ. Figure 3, *a* shows the experimental emission spectrum obtained by rotating the fiber by angle ϑ for sample No. 1 (Fig. 2, *a*) and the calculated CR spectrum obtained by modelling with the GEANT4 code. Figure 3, *a* reveals a fairly good match between the experimental and calculated CR spectra. In addition, the experimental and calculated angular dependences of CR intensity at a wavelength of 326 nm on the fiber rotation angle were obtained (Fig. 3, *b*). The wavelength of 326 nm was chosen arbitrarily in the UV region of the

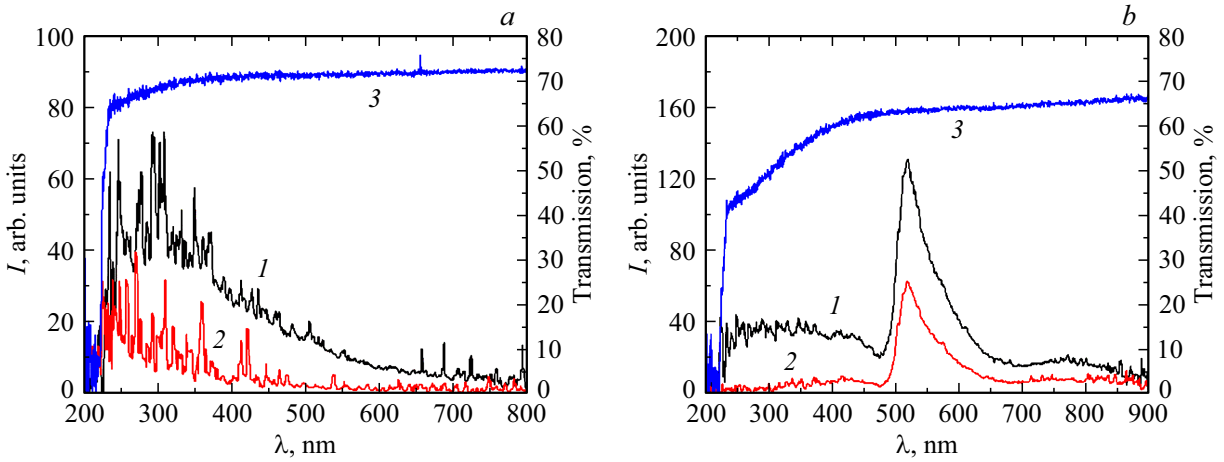

Figure 2. Emission (*1, 2*) and transmission (*3*) spectra of samples Nos. 1 (*a*) and 2 (*b*) measured with the fiber rotated by angle ϑ (curve *1*) and φ (curve *2*).

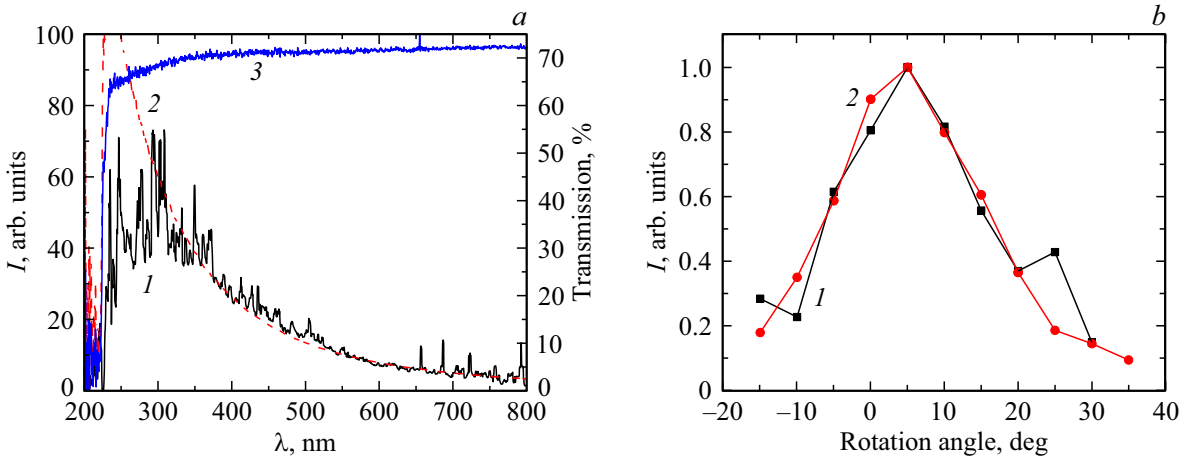

Figure 3. *a* — Emission (*1*), transmittance (*3*), and calculated CR (*2*) spectrum for sample No. 1; *b* — experimental (*1*) and calculated (*2*) angular dependences of the CR intensity on the fiber rotation angle at a wavelength of 326 nm. Sample No. 1.

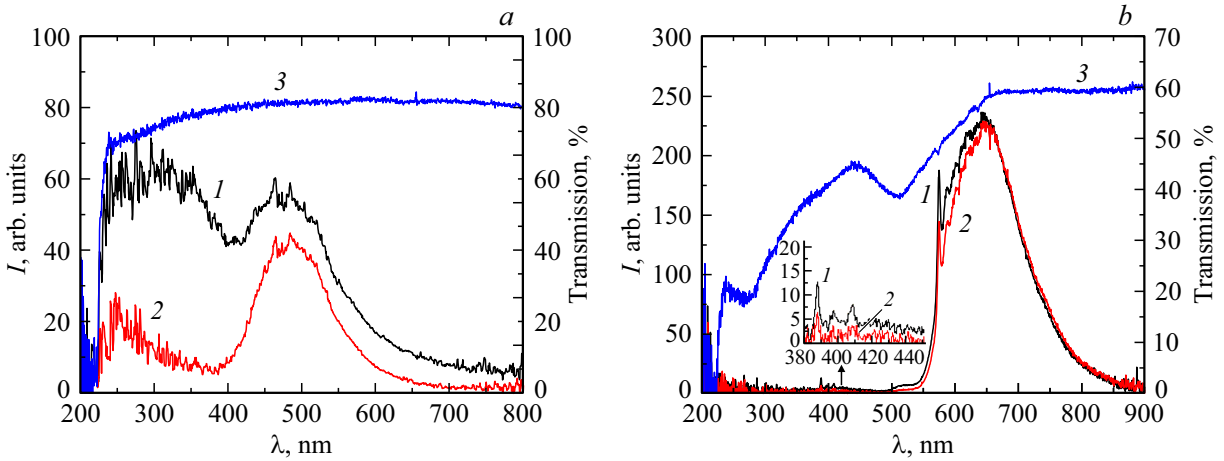

Figure 4. Emission (*1, 2*) and transmission (*3*) spectra of samples Nos. 3 (*a*) and 4 (*b*) measured with the fiber rotated by angle ϑ (curve *1*) and φ (curve *2*).

spectrum where the intensity of CR reaches its maximum. The angular dependence was also calculated in GEANT4. Positive angles in Fig. 3, *b* correspond to clockwise rotation of the fiber from axis *Y* toward angle ϑ; negative angles, to counterclockwise rotation of the fiber from axis *Y* toward angle φ. Figure 3, *b* reveals a good match between the calculated and experimental angular dependences of CR intensity, which further confirms that this radiation is CR by nature.

It is important to note that the luminescence of excitons with an intense band at 235 nm was observed in [6] in the emission spectra of the same sample (No. 1) exposed to an electron beam of lower energy (up to 300 keV) but higher current density (~ 100 A/cm^2). We believe that the emergence of the exciton band depends on the beam current density, since exciton luminescence is a quadratic process of recombination of electron–hole pairs and its intensity depends nonlinearly on the excitation density.

In the emission spectrum of sample No. 2 (Fig. 2, *b*), a zero-phonon line (ZPL) at 503 nm and a broad luminescence band in the wavelength range of 480–650 nm with a maximum at 519 nm, which is associated with N_2V^0 centers and is the vibronic system H3 [14], are observed against the background of CR. At angle ϑ optimum for CR detection, the emission intensity starts increasing with decreasing wavelength in the UV region of the spectrum (Fig. 2, *b*, curve *1*), which is a confirmation of the presence of CR in the emission spectrum of this sample. At wavelengths shorter than 400 nm, the growth of CR intensity slows down, which is explained by the increase of absorption in the transmission spectrum of this sample in this spectral range (Fig. 2, *b*, curve *3*). When the fiber is rotated by angle φ, CR is also observed in the emission spectrum of sample No. 2, but its intensity decreases noticeably at wavelengths shorter than 400 nm (Fig. 2, *b*, curve *2*), since the number of CR photons reaching the fiber is much smaller at this rotation angle.

In contrast to the spectrum of nominally pure sample No. 1, the emission spectrum of nominally pure sample No. 3 (Fig. 4, *a*) features a broad luminescence band in the 400–700 nm wavelength range, which is apparently the A-band [14], in addition to CR.

In the emission spectra at angle ϑ optimum for CR detection, a sharp rise in the emission intensity with decreasing wavelength is observed (Fig. 4, *a*, curve *1*); when the fiber is rotated by angle φ, the growth of CR intensity becomes not so sharp (Fig. 4, *a*, curve *2*). Just as in sample No. 1, no exciton cathodoluminescence was observed in the emission spectra of this nominally pure sample.

The emission spectrum of sample No. 4 (Fig. 4, *b*) shows intense luminescence of an NV^0 center with ZPL at 575 nm and its phonon replicas. In addition, the shape of transmission spectra in the range of 500–700 nm and emission spectra in the range of 500–900 nm (Fig. 4, *b*) suggests that the emission of NV^- centers is also realized in this sample due to the self-absorption of luminescence of NV^0 centers. Also, the emission spectrum of this sample exhibits an vibronic system due to its own interstitial atoms, with ZPL at 389 nm and phonon replicas in the range of 390–450 nm. No Cherenkov radiation was observed in this sample against the background of an intense cathodoluminescence band and stronger absorption in the UV region of the spectrum.

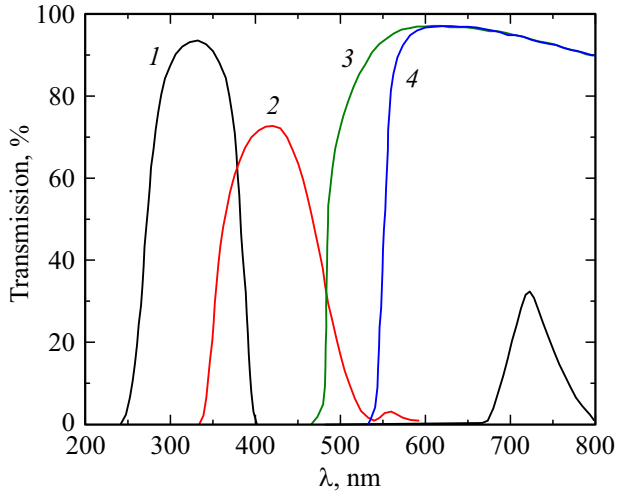

Figure 5. Transmission spectra of UFS-2 (*1*), SS-8 (*2*), ZhS-17 (*3*), and OS-12 (*4*) optical filters.

Kinetic characteristics of emission of diamond samples

In experiments on measurement of kinetic characteristics of emission, various optical filters were used to select the necessary spectral range. Their transmission spectra are shown in Fig. 5. These optical filters were selected based on the obtained spectral data on emission of diamond samples (Figs. 2–4). The long-wavelength boundary of the spectral range in which emission pulses from the PMT were recorded for optical filters ZhS-17 and OS-12 was limited by the long-wavelength boundary of the PMT sensitivity band, which was 900 nm.

The shape of emission pulses recorded by the PMT varied from pulse to pulse, which is associated with a certain instability of the microtron operation. Figure 6 shows the emission pulses for sample No. 1 obtained with the PMT at different angles of rotation of the fiber. When recording the emission pulses, a UFS-2 optical filter was used to isolate the UV region of the spectrum in which the CR spectrometer operated (Figs. 2, *a* and 3). When the fiber was rotated by angle φ, which was suboptimal for CR detection, the PMT signal level decreased markedly (Fig. 6, *b*). The number of electrons of the beam, which was monitored by the induction current sensor, practically did not change (the difference was no more than 5%) during the recording of emission pulses (Figs. 6, *a* and *b*).

The durations of emission pulses at different angles of fiber rotation (Fig. 6) approximately corresponded to the duration of the microtron beam current macropulse

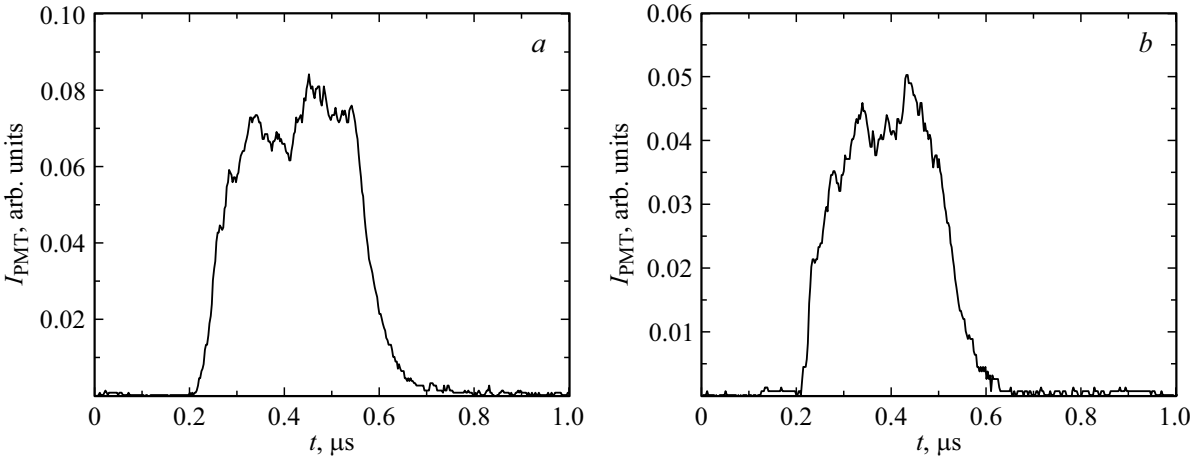

Figure 6. Emission waveforms of emission for sample №. 1 obtained with the fiber rotated by angle ϑ (a) and φ (b). UFS-2 optical filter.

($\sim 0.5\,\mu$s). The difference in full width at half maximum (FWHM) emission pulse durations was less than 50 ns, which corresponded to the variation of the microtron beam current duration (no more than 10%).

UFS-2 (260–380 nm) and ZhS-17 (480–3000 nm) optical filters were used to record the emission pulses for sample No. 2. CR in the UV region of the spectrum was highlighted using a UFS-2 light filter, and emission of the broad luminescence band (Fig. 2, b), which is associated with N_2V^0 centers, was highlighted using a ZhS-17 light filter. When recording the emission pulses in the 480–900 nm range (Fig. 7, b), a high PMT signal level was observed, so the current had to be significantly reduced (by a factor of ~ 10) to prevent the PMT from entering the saturation mode. The PMT signal in the spectral range of 480–900 nm (Fig. 7, b), even when the current was reduced ~ 10 times, was significantly higher (~ 10 times) than the signal level recorded in the UV region of the spectrum (Fig. 7, a). The FWHM CR pulse duration (Fig. 7, a) was 266 ns, while the FWHM pulse duration for emission of N_2V^0 centers was 177 ns (Fig. 7, b). The decay of the CR pulse, which is an inertia-free process [3], is due to the decay of the pulse response of the PMT used. The characteristic time of exponential decay of the CR pulse was 43 ns, which agrees well with the microcells recharge time constant of this PMT (45 ns [13]). For the emission pulse of N_2V^0 centers, the characteristic exponential decay time was 53 ns. Taking into account a significant reduction in the FWHM duration of the emission pulse and an increase in the exponential decay time compared to the CR pulse, it can be assumed that luminescence quenching occurs in the process of cathodoluminescence of N_2V^0 centers during excitation by an electron beam with an energy of several MeV and a duration of several hundred nanoseconds. This effect can be explained by a change in the charge state of N_2V^0 centers due to trapping of secondary charge carriers, which, however, requires a separate study beyond the scope of this work.

Emission pulses for low-impurity diamond sample No. 3 (Fig. 8) were recorded in two spectral ranges. A UFS-2 light filter was also used to record the CR pulses in the UV region of the spectrum. To record the emission pulses of a wide luminescence band, which appears to be the A-band (Fig. 4, a), an SS-8 light filter was used. The PMT signal level obtained with the SS-8 light filter (Fig. 8, a), which highlights the ~ 360–540 nm spectral range (Fig. 5), is more than 3 times lower than the PMT signal level in the UV region of the spectrum (Fig. 8, b). The number of beam electrons did not change during the recording of emission pulses (Figs. 8, a and b). The durations of emission pulses in two spectral ranges (Figs. 8, a and b) are approximately consistent with each other. The difference in FWHM emission pulse durations for this sample was also less than 50 ns (just as for sample No. 1). This correlated with the variation of the microtron beam current duration, which was no more than 10%.

Figure 9 shows the waveforms of emission in different spectral ranges for sample No. 4. The number of beam electrons was practically unchanged when these records were obtained (the difference was no more than 5%). In the UV region of the spectrum, emission (Fig. 9, a), which is Cherenkov radiation, was recorded; notably, CR was not detected against the background of an intense cathodoluminescence band in emission spectra (Fig. 4, b). An SS-8 light filter (Fig. 5) was used to record the emission pulses of ZPL at 389 nm and its phonon replicas emitting in the 390–540 nm range (Fig. 4, b). The PMT signal level in this spectral range (Fig. 9, b) was more than 2 times higher than the signal level in the UV spectral region (Fig. 9, a). An OS-12 light filter (Fig. 5) was used to record the emission of NV^0 centers with ZPL at 575 nm in this sample (Fig. 9, c).

The emission intensity detected by the PMT in this spectral range (540–900 nm) is much higher than the emission intensity in the spectral ranges highlighted by SS-8 (Fig. 9, b) and UFS-2 (Fig. 9, a) filters. In addition, the emission duration of NV^0 centers (Fig. 9, c) was much longer than that in other spectral bands (Figs. 9, a and b).

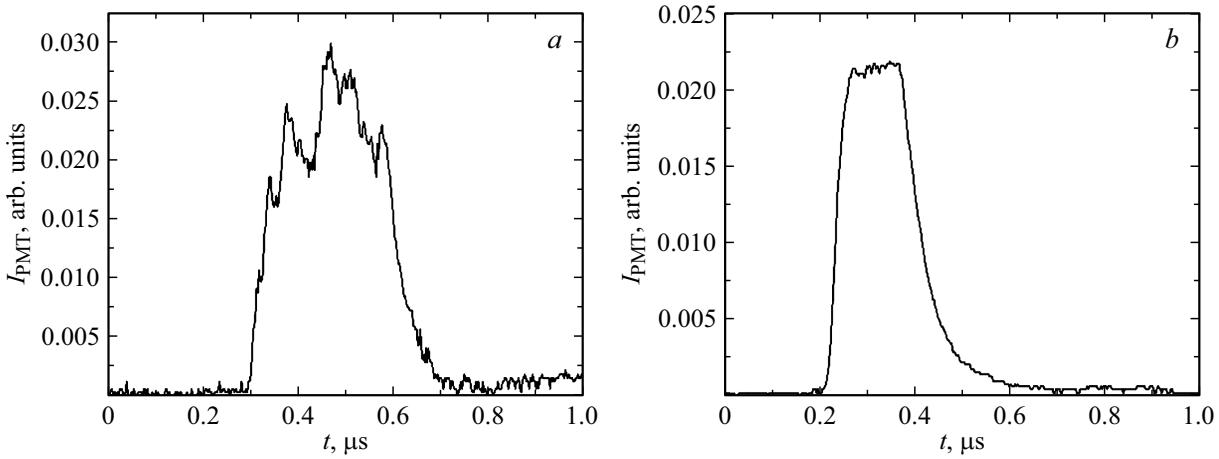

Figure 7. Waveforms of emission for sample No. 2 measured with the fiber rotated by angle ϑ using a UFS-2 filter (a) and by angle φ using a ZhS-17 filter (b).

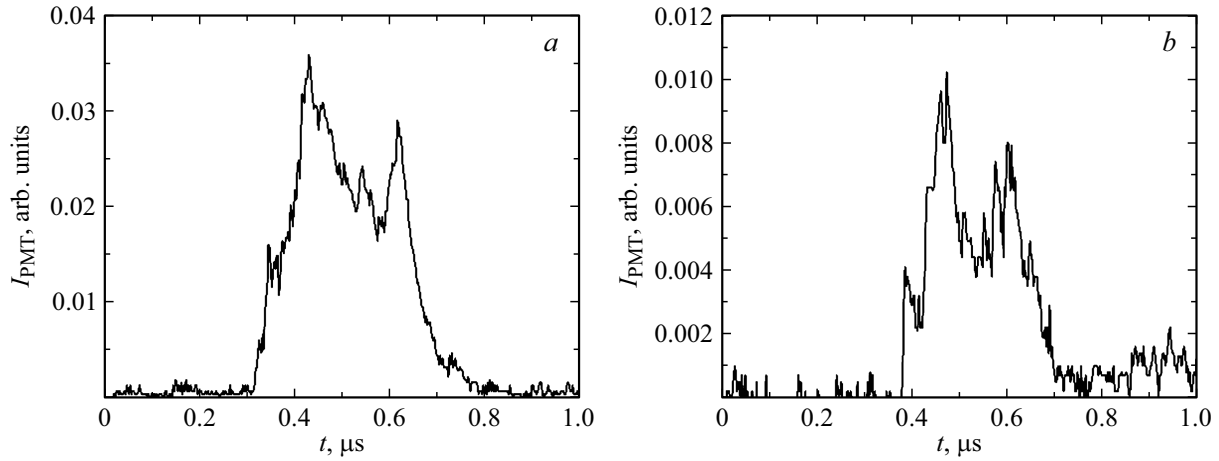

Figure 8. Waveforms of emission for sample No. 3 measured with the fiber rotated by angle φ using a UFS-2 filter (a) and by angle φ using an SS-8 filter (b).

The corresponding characteristic time of exponential decay of the longest component was 964 ns, which exceeds significantly the literature data ($\sim$ 30 ns for NV^0 centers [14]).

This fact indicates a possible contribution of other luminescence centers to CL, which also warrants a separate study.

Conclusion

The spectral-kinetic characteristics of emission of diamond samples with different impurity-defect compositions fabricated by temperature gradient and chemical vapor deposition methods have been studied. Cherenkov radiation was obtained in all the studied diamond samples. For sample No. 4, CR could be recorded using a PMT and a light filter that cut off the intense cathodoluminescence of NV^0 centers. The study of luminescence kinetics showed that luminescence of an uncertain nature is present in the spectral range of 540−850 nm in addition to the emission of NV^0 centers.

In the emission spectra of sample No. 2, a broad luminescence band in the wavelength range of 480-650-nm, which is the vibronic system H3, was observed in addition to CR. The reduction in emission duration of this luminescence band compared to the duration of CR in this sample can be explained by the change in the charge state of N_2V^0 centers upon trapping of secondary electrons, which leads to a change in the position of the Fermi level, a change in the charge state to N_2V^-, and quenching of the luminescence band of N_2V^0 centers. However, this assumption requires further research.

The emission spectra for nominally pure samples Nos. 1 and 3 were very different, which is apparently due to the difference in synthesis methods. In sample No. 3, which was obtained by HPHT synthesis, a broad luminescence band in the emission spectrum in the wavelength range of 400−700 nm, which is presumed to be the A-band, was observed in addition to CR. In addition, luminescence of free excitons was lacking in the emission spectra of samples Nos. 1 and 3. This luminescence was observed when

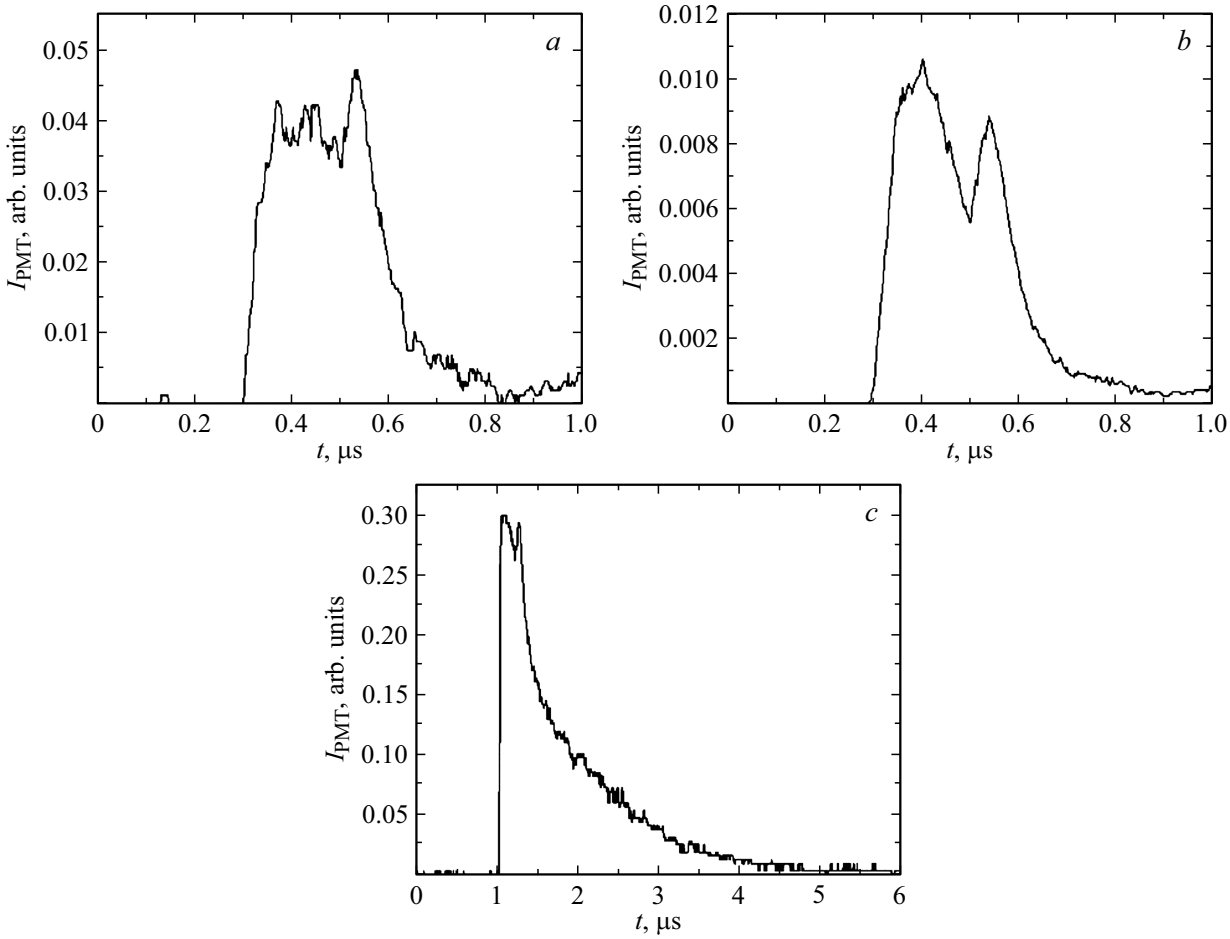

Figure 9. Waveforms of emission for sample No. 4 measured with the fiber rotated by angle ϑ using a UFS-2 filter (*a*) and by angle φ using SS-8 (*b*) and OS-12 (*c*) filters.

exposed to a beam of electrons with lower energy (up to 300 keV) but higher beam current density (~ 100 A/cm^2), which is apparently related to the dependence of the emission intensity of free excitons on the excitation density.

The results of calculations of CR generation in diamond with the GEANT4 numerical code are in good agreement with the experimental data. Nominally pure sample No. 1, which lacked luminescence, is a promising radiator material for building a Cherenkov detector capable of operating in conditions of relatively low concentrations of charged particles (electrons), such as near-Earth space.

Acknowledgments

The authors would like to thank E.Kh. Baksht, S.R. Uglov, and M.V. Shevelev for their participation in discussion of the results of this work.

Funding

This study was supported by the Russian Science Foundation, grant № 22-22-00984, https://rscf.ru/project/22-22-00984/.

Conflict of interest

The authors declare that they have no conflict of interest.

References

[1] J.F. Hochedez, P. Bergonzo, M.-C. Castex, P. Dhez, O. Hainaut, M. Sacchi, J. Alvarez, H. Boyer, A. Deneuville, P. Gibart, B. Guizard, J.-P. Kleider, P. Lemaire, C. Mer, E. Manroy, E. Munoz, P. Muret, F. Omnes, J.L. Pau, V. Ralchenko, D. Tromson, E. Verwichte, J.-C. Vial. Diamond and Related Materials, **10** (3–7), 673 (2001). DOI: 10.1016/S0925-9635(01)00374-0

[2] M.J. Sadowski. Nukleonika, **56** (2), 85 (2011).

[3] V.P. Zrelov. *Izluchenie Vavilova–Cherenkova i ego primenenie v fizike vysokikh energii* (Atomizdat, M., 1968) (in Russian).

[4] A.M. Gal'per. Soros. Obraz. Zh., (6), 75 (1999) (in Russian).

[5] A.G. Burachenko, V.S. Ripenko, E.I Lipatov, K.P. Artyomov, A.A. Krylov. Russ. Phys. J., **65**, 1812 (2023). DOI: 10.1007/s11182-023-02835-1.

[6] A.G. Burachenko, D.A. Peresedova, A.A. Krylov, V.S. Ripenko, E.I. Lipatov, K.P. Artemov. In Proc. Of 8th Int. Cong. EFRE (Tomsk, 2022), p. 1494. DOI: 10.56761/EFRE2022.N4-O-909501

[7] R.A. Khmel'nitskii, N.Kh. Talipov, G.V. Chucheva. *Sintetich-eskii almaz dlya elektroniki i optiki* (Ikar, M., 2017) (in Russian).
[8] V.I. Gridev, E.I. Rozum, A.M. Slupskii, S.A. Vorob'ev. Prib. Tekh. Eksp., (1), 20 (1987) (in Russian).
[9] B.A. Alekseev, A.V. Vukolov, F.V. Konusov, S.K. Pavlov, A.P. Potylitsyn, S.R. Uglov, Yu.M. Cherepennikov, M.V. Shevelev, A.G. Burachenko. Phys. Part. Nucl. Lett., **20** (1), 38 (2023).
[10] V.F. Tarasenko, E.Kh. Baksht, M.V. Erofeev, A.G. Burachenko. Opt. Spectrosc, **129** (7), 707 (2021). DOI: 10.21883/OS.2021.05.50883.310-20
[11] E.Kh. Baksht, B.A. Alekseev, A.G. Burachenko, A.V. Vukolov, A.P. Potylitsyn, V.F. Tarasenko, S.R. Uglov, M.V. Shevelev. Matter Radiat. Extremes, **7** (2), 026901 (2022). DOI: 10.1063/5.0061100
[12] S. Agostinelli (Geant4 Collaboration) et al. Nuclear Instruments and Methods in Physics Research Section A: Accelerators, Spectrometers, Detectors and Associated Equipment, **506** (3) 250 (2003). DOI: 10.1016/S0168-9002(03)01368-8
[13] MICROJ-SERIES - Silicon Photomultipliers (SiPM), High PDE and Timing Resolution Sensors in a TSV Package [Electronic source]. URL:https://www.onsemi.com/download/data-sheet/pdf/microj-series-d.pdf
[14] A.M. Zaitsev. *Optical properties of diamond: a data handbook*, 1st ed. (Springer, Berlin, Heidelberg, 2013). DOI: 10.1007/978-3-662-04548-0

Translated by D.Safin